ELSEVIER

Journal of Nuclear Materials 313–316 (2003) 1046–1051

journal of nuclear materials

www.elsevier.com/locate/jnucmat

Observation of molecular assisted recombination via negative ions formation in a divertor plasma simulator, TPDSHEET-IV

Akira Tonegawa [a,*], Masataka Ono [b], Yasushi Morihira [a], Hironori Ogawa [a], Takehisa Shibuya [c], Kazutaka Kawamura [d], Kazuo Takayama [d]

[a] *Department of Physics, School of Science, Tokai University, 1117 Kitakaname, Hiratsuka, Kanagawa 259-1292, Japan*
[b] *Department of Nuclear Energy, School of Engineering, Tokai University, 1117 Kitakaname, Hiratsuka, Kanagawa 259-1292, Japan*
[c] *Department of Electro-Photo Optics, School of Engineering, Tokai University, 1117 Kitakaname, Hiratsuka, Kanagawa 259-1292, Japan*
[d] *Research Institute of Science and Technology, Tokai University, 1117 Kitakaname, Hiratsuka, Kanagawa 259-1292, Japan*

Abstract

Molecular assisted recombination (MAR) via negative ions formation has been observed in a linear plasma simulator. A small amount of hydrogen gas puffed into a hydrogen plasma strongly reduced the heat flux to the target and rapidly increased the density of negative ions of hydrogen atom, n_{H^-}, in the circumference of the plasma, while the conventional radiative and three-body recombination processes disappeared. n_{H^-} is localized in the outer region where electrons exist ($n_e \sim 5 \times 10^{17}$ m^{-3}, $T_e = 3$–5 eV). The peak value of n_{H^-} is 1.2×10^{17} m^{-3} and the ratio of n_{H^-}/n_e in the outer region goes up to over 20%. These results can be well explained by taking the mutual neutralization between the negative and positive ions of MAR in the detached plasma into account.

PACS: 52.40.−w; 52.20.Hv; 52.70.−m; 25.20.H
Keywords: Divertor; Molecular assisted recombination; Negative ion; Detached plasma; Laser photodetachment; Sheet plasma

1. Introduction

Recent experiments on divertor tokamaks [1,2] and divertor simulators [3–6] have focused on the studies of molecular and atomic processes under the detached divertor regimes. Until quite recently, researches primarily have dealt with plasma momentum/pressure loss which is based on such plasma–neutral interactions as the radiative and three-body recombination, that is, electron-ion recombination (EIR). However, it is difficult from the view of only EIR to explain the loss in plasma particle flux at the plates that occurs as well [7]. In fusion experiments with a detached plasma, the plasma recombines before it reaches the targets. Such recombination is the only process allowing to reduce plasma flux at the target plate in fusion experiments without a strong impurity radiation loss of EIR [8,9].

The importance of other recombination processes associated with molecular reactions, such as the molecular assisted recombination (MAR) involving a vibrationally excited hydrogen molecule, has been emphasized in theoretical investigation and modeling [8,10–12]. In fusion related experiments there are two main paths for MAR: (1) $H_2(v) + e \Rightarrow H^- + H$ (dissociated attachment) followed by $H^- + H^+ \Rightarrow H + H(n = 3)$ (mutual neutralization), and (2) $H_2(v) + A^+ \Rightarrow (AH)^+ + H$ (ion conversion) followed by $(AH)^+ + e \Rightarrow A + H$ (dissociative recombination), where $A^+(A)$ is a

* Corresponding author. Tel.: +81-463 58 1211x3710; fax: +81-463 50 2013.
E-mail address: tone@keyaki.cc.u-tokai.ac.jp (A. Tonegawa).

0022-3115/03/$ - see front matter
PII: S0022-3115(02)01535-0

hydrogen or an impurity ion (atom) existing in divertor plasma. MAR is expected to enhance the reduction of ion particle flux, and to modify the detached recombining plasmas because the rate coefficient for MAR is much greater than that one for EIR at relatively electron temperatures above 1.0 eV. Especially, it was noted from theoretical considerations that the formation of negative ions due to the successive breakup of molecules might open a new channel for recombination under certain conditions [12]. The rate coefficient of such mutual neutralization between the positive and negative ions in MAR is about a factor 30 of magnitude larger than the ones for EIR rate coefficients at various electron temperatures [13–15]. Therefore, the negative ion plays an important role in the mutual neutralization of MAR. We have carried out the experiment to show that the huge amount of ion particle and heat fluxes at the plasma-facing components in next generation fusion device intended for a long pulse or steady state operation could possibly be controlled by the regulation of the negative ion density in a detached plasma.

However, the role of the MAR in fusion experiments is still under discussion and various conclusions are derived from the analysis of different experiments [8,9]. One of the experimental results of the spectroscopy in the linear plasma simulator has provided the evidence of dissociative recombination in MAR, showing the reduction of the ion flux in a plasma with a hydrogen/helium mixture [4]. On the other hand, other experiments, gave ambiguous results because it does not choose most predominant recombination between the mutual neutralization and the dissociative recombination. It is, thus, required that the experiments which will be essential to an understanding of the role of the negative ions come out. In MAR negative ions of hydrogen atom have not reported in the detached plasma which is observed in diverted tokamaks and divertor simulators.

In this paper, we present the first experimental observation of the mutual neutralization in MAR via negative ions formation of hydrogen atom for hydrogen detached plasma in the linear divertor plasma simulator, TPDSHEET-IV (test plasma produced by directed current for SHEET plasma) [16,17]. Measurements of the negative ion density of hydrogen atom n_{H^-}, the electron density n_e, electron temperature T_e, and the heat load to the target plate Q were carried out in hydrogen detached plasma with hydrogen gas puff. It is also intended to show that the observed hydrogen Balmer spectra could be explained by EIR.

2. Experimental apparatus and method

The experiment was performed in the linear divertor plasma simulator TPDSHEET-IV as shown in Fig. 1. The plasma in TPDSHEET-IV was divided into two regions: the sheet plasma source region and the experimental region for divertor simulator. The hydrogen sheet plasma was produced by a modified TP-D type dc discharge [18]. The anode slit was 2 mm thick and 40 mm wide. Ten rectangular magnetic coils formed a uniform magnetic field of 0.7 kG in the experimental region. The sheet plasma was terminated by the electrically floating and water-cooled target plate (stainless steel) axially positioned of $z = 0.7$ m away from the discharge anode electrode. The hydrogen plasma was generated at a hydrogen gas flow of 70 sccm with a discharge current of 50 A. The neutral pressure P_{Div} in the divertor test region was controlled by feeding a secondary gas from 0.1 to 20 mTorr. The change of P_{Div} in the divertor test region had no effect on the plasma production in the discharge region because the pressure difference between the discharge and divertor test regions extends to three orders of magnitude. The electron temperature and the electron density were measured by a plane Langmuir probe. The plane Langmuir probe was located 3 cm apart from the target plate. The power on the target plate, Q was measured by calorimeter. A cylindrical probe made of tungsten ($\varnothing 0.4 \times 2$ cm) was used to measure the spatial profiles of H^- by a probe-assisted laser photodetachment method [19,20]. The maximum lager energy at the fundamental wavelength (1064 nm) was 100 mJ. The pulse length was about 10 ns and the diameter of the beam was 8 mm. The negative ion density was determined from the photodetached electron current. The spatial profile of the negative ions was measured by moving the cylindrical probe under the laser irradiation. The Balmer spectra of visible light emission from the hydrogen atoms were detected 3 cm apart from the target plate. The analysis of the Balmer line intensities show that the upper levels of these transitions are populated primarily by radiative recombination [21]. Also, the intensities of the lines of the Balmer series, such as the $5 \rightarrow 2(H_\gamma)$, are directly related to the recombination rate of EIR. Therefore the intensity ratio of the H_γ to the $H_\alpha(3 \rightarrow 2)$ line can be used as an EIR indicator, where the H_α line is considered as the one related to the mutual neutralization between the negative and positive ions mentioned before [22].

3. Experimental results and discussion

Fig. 2 shows the spatial profiles of n_{H^-}, n_e, and T_e in the y-direction at various P_{Div}. At $P_{Div} \sim 0.8$ mTorr, both T_e and n_e have hill-shaped profiles with a half width for T_e and n_e of about ± 2.5 mm and ± 5.0 mm for the sheet plasma, respectively. The produced sheet plasma has a steep electron temperature gradient over the narrow space of several centimeters: the hot plasma ($\sim$15 eV) in the central region and the cold plasma (3–5 eV)

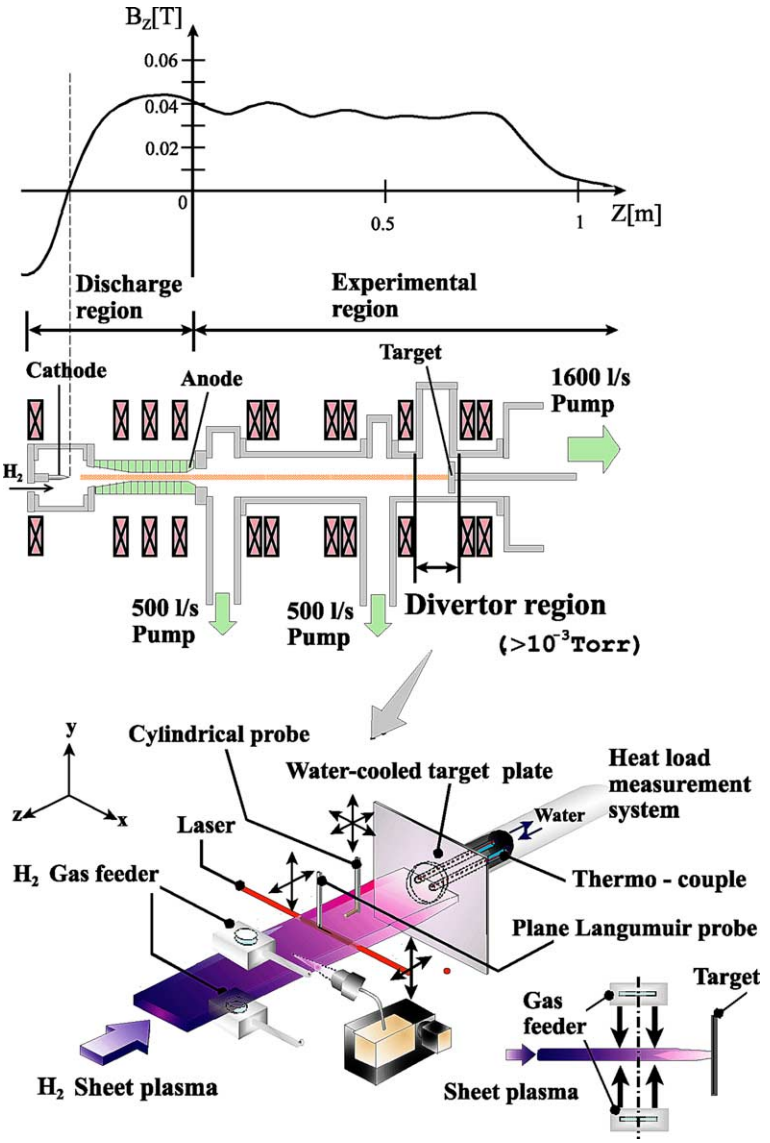

Fig. 1. Schematic diagram of the magnetized plasma simulator (sheet plasma device) TPDSHEET-IV and detection system. The profile of the axial magnetic field B_z is shown in the upper part.

in the outer region. At a small amount of secondary hydrogen gas puffing into a hydrogen plasma, n_{H^-} is localized in the outer region ($y = 10$–20 mm) where cold electrons ($n_e \sim 5 \times 10^{17}$ m^{-3}, $T_e = 3$–5 eV) come from the circumference of the plasma exist. The peak value of n_{H^-} is 4×10^{16} m^{-3} and is less than one order of that of the electron density in the outer region. At $P_{Div} \sim 3.5$ mTorr, the peak value of n_{H^-} is 1×10^{17} m^{-3} and the ratio of n_{H^-}/n_e in the outer region goes up to over 20%. In this condition, the ion–neutral and electron–neutral collision mean free path are a few centimeters for this gas pressure. Also, the dissociative-attachment cross-sections for the metastable molecules at the vibrationally excited state $\upsilon = 4$, are four orders of magnitude larger than those for the vibrationally ground state $\upsilon = 0$ [23]. Therefore, the negative ion production by dissociative electron attachment is enhanced when the hydrogen molecule is vibrationally excited in the detached plasma. Further increase of P_{Div}, both T_e of the central region and n_{H^-} in the outer region gradually decrease.

Fig. 3 shows the dependence of Q to the target plate, the hydrogen Balmer line intensity ratio H_γ/H_α, the electron density n_{ec} and temperature T_{ec} at the center of sheet plasma, and n_{H^-} on hydrogen gas pressure P_{Div}.

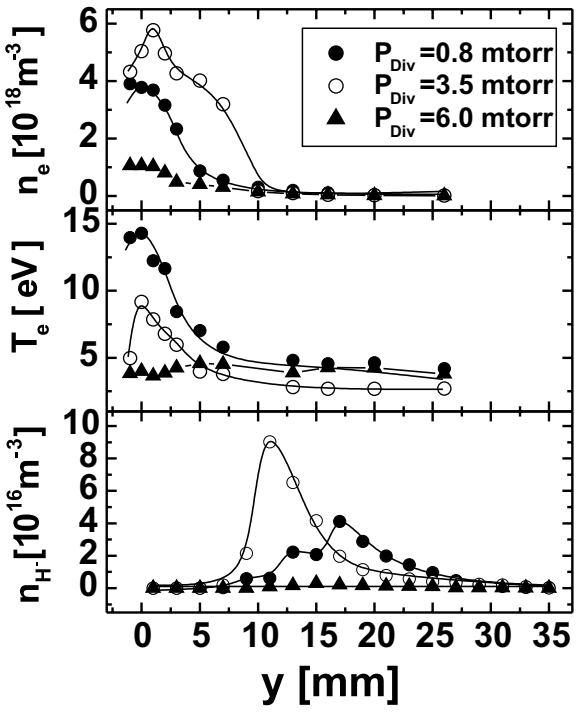

Fig. 2. Spatial profiles in the y-direction of the negative ion density of n_{H^-}, the electron temperature T_e, and the electron density n_e for three different hydrogen gas pressures P_{Div} of 0.8 (solid circles), 3.5 (open circles), and 6 (solid triangles) mTorr.

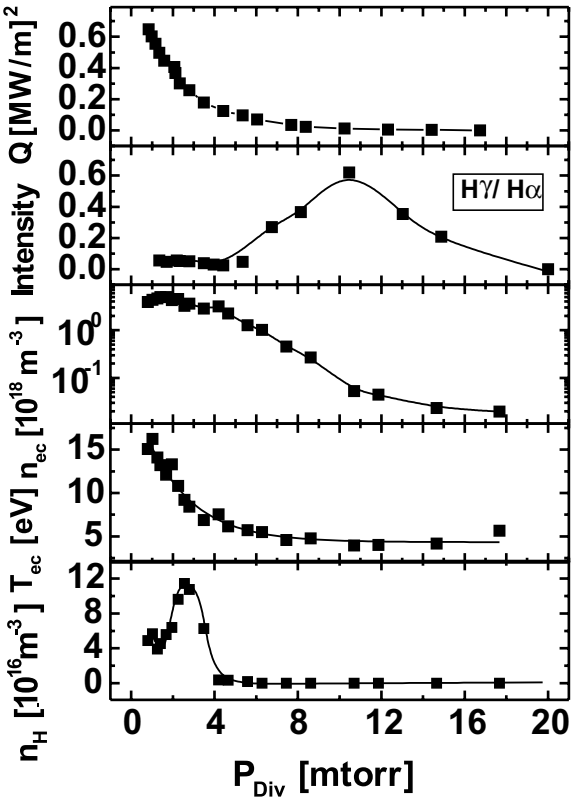

Fig. 3. Averaged heat load to the target plate Q, and the hydrogen Balmer intensity ratio H_γ/H_α, the electron density n_{ec}, and the electron temperature T_{ec} in the center of the plasma, the negative ion density of n_{H^-} as a function of the hydrogen gas pressure P_{Div} in the divertor test region.

With increasing in P_{Div}, the value of Q is found to decrease rapidly, until less than 30% of the initial value of $P_{Div} \sim 3$ mTorr. T_{ec} decreases rapidly from 15 to 8 eV and the peak value of n_{H^-} is 1.2×10^{17} m^{-3}. On the other hand, n_{ec} increases slightly from 4×10^{18} to 6×10^{18} m^{-3} until $P_{Div} \sim 3$ mTorr due to ionization, while Balmer line intensity ratio H_γ/H_α remains constant. Above $P_{Div} \sim 3$ mTorr in which T_{ec} is less than ~8 eV, we can observe a sudden drop from 6×10^{18} m^{-3} to several 10^{16} m^{-3} in n_{ec} and a rapid increase of the maxima in the photon ratio of H_γ/H_α. At the same time, the line intensities of the Balmer series ($n = 7$–16) influenced by EIR were observed in front of the target as shown in Fig. 4. In the detached plasma experiments, the plasma recombines before it reaches the target and such recombination is the only process allowing the reduction of both plasma flux and heat flux at the wall without strong impurity radiation loss. As a result, it is noted that the detached plasma is achieved by a small amount of secondary hydrogen gas puffing into a hydrogen plasma, although the conventional processes were quenched. Moreover, very bright visible light emission in front of the target plate, were observed in the detached plasma. A further increase in P_{Div} leads to keep the bright emission region

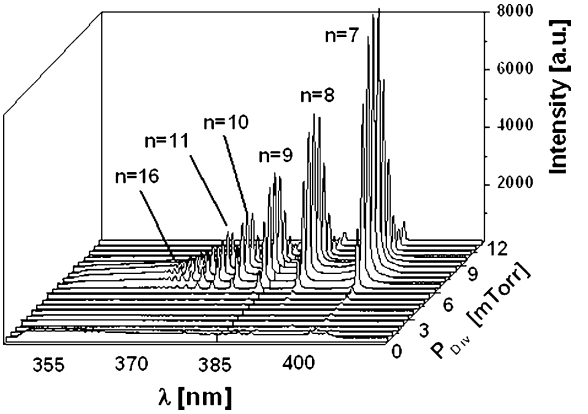

Fig. 4. Visible light emission spectra from a hydrogen plasma with a hydrogen gas puff.

(full detachment region) far apart from the target plate, then it appears a clear dark region between the target

plate and the region with the bright visible emissions, resulting the rapid decrease of the photon ratio H_γ/H_α. This channel corresponds to the radiation and three-body recombination as EIR.

The plasma recombination time, τ_{MAR}, related to the mutual neutralization is given by $\sim(\nu_{MAR})^{-1}$, where $\nu_{MAR} = \langle\sigma v\rangle_{MAR} n_{H^-}$ (ν_{MAR} is rate coefficient of MAR and n_{H^-} is negative ion density of hydrogen atom). For $P_{Div} \sim 3$ mTorr, $n_{H^-} \sim 1.2 \times 10^{17}$ m^{-3}, and $\langle\sigma v\rangle_{MAR} \sim 4 \times 10^{-14}$ m^3/s, we can estimate τ_{MAR} to be 2×10^{-4} s. Then, the plasma ion flow time scale is given by $\tau_i \sim L/u_i$, where L is the length of the plasma in the divertor test region and u_i is the ion flow velocity. Here, τ_i means the translational time of an ion generated in the plasma source region towards the target plate. We have $u_i \sim c_s (\lambda_{in}/L)$, where λ_{in} is the ion mean free path till ion–neutral collision, that is, $\lambda_{in} \sim 1/n_n\sigma_{in}$ (n_n is the neutral density and σ_{in} is the ion–neutral collision cross-section), and $c_s \sim (T_e/M_i)^{0.5}$ (c_s is sound velocity and M_i is the ion mass). For $L \sim 1$ m, $T_e \sim 4$ eV, $n_n \sim 10^{20}$ m^{-3}, $\sigma_{in} \sim 10^{-18}$ m^{-2}, we get $\tau_i \sim 5 \times 10^{-3}$ s. The plasma recombination time scale for EIR τ_{EIR} is determined by $\tau_{EIR} \sim (\nu_{EIR})^{-1}$, where $\nu_{EIR} = \langle\sigma v\rangle_{EIR}\ n_e$ ($\langle\sigma v\rangle_{EIR}$ is rate coefficient of EIR). For our experimental conditions, τ_{EIR} may vary from 10^{-1} s to 10^{-2} s depending on T_e and n_e. The above scalings mean that MAR has strong influence on recombination at small gas pressures because τ_{MAR} becomes smaller than the time scales for τ_i and τ_{EIR}. This means that it is more probable that recombination processes are based on MAR via negative hydrogen ions. It is suggested from the present experimental results that MAR plays an important role in plasma recombination under typical conditions of a detached plasma.

4. Conclusion

We have observed MAR via negative ion formation in a detached hydrogen plasma by using a linear plasma simulator. When a small amount of secondary hydrogen gas is puffed into the hydrogen plasma, the density of negative hydrogen ions in the circumference of the plasma rapidly increases and a strong reduction of the heat flux to the target is observed without both the very bright visible light emission and three-body recombination as EIR. These results can be well explained by taking the charge exchange recombination of MAR in the detached plasma into account. Our experimental results could be useful to control the divertor operation and to determine the optimum conditions for a detached plasma production, since the complex phenomena involving the collision with hydrogen molecules and negative ions in MAR are elucidated through the present research.

Acknowledgements

This work is part of a program supported by the LHD Joint Project, the National Institute for Fusion Science.

References

[1] H. Hutchinson, R. Boivin, F. Bombarda, P. Bonoli, S. Fairfax, C. Fiore, J. Goetz, S. Golovato, R. Granetz, M. Grenwald, S. Horne, A. Hubbard, J. Irby, B. LaBombard, B. Lipschultz, E. Marmar, G. McCracken, M. Porkolab, J. Rice, J. Snipes, Y. Takase, J. Terry, S. Wolfe, C. Christensen, D. Garnier, M. Graf, T. Hsu, T. Luke, M. May, A. Nemczewski, G. Tinios, J. Schachterm, J. Urban, Phys. Plasma 1 (1994) 1511.
[2] T.W. Petrie, D. Buchenauer, D.N. Hill, C. Klepper, S. Allen, R. Campbell, A. Futch, R.J. Groebner, A. Leonard, S. Lippmann, M. Ali Mahdavi, M. Rensink, P. West, J. Nucl. Mater. 196–198 (1992) 848.
[3] L. Schmitz, B. Merriman, L. Blush, R. Lehmer, R.W. Comm, R. Doemer, A. Grossman, F. Najmabadi, Phys. Plasma 2 (1995) 3081.
[4] N. Ohno, N. Esumi, S. Takamura, S.I. Krasheninnikov, Yu. Pigarov, Phys. Rev. Lett. 81 (1998) 818.
[5] G.S. Chiu, S.A. Cohen, Phys. Rev. Lett. 76 (1996) 1248.
[6] E.S. Nektarov, V.B. Petrov, V.V. Sychev, B.I. Khripunov, V.V. Shapkin, G.V. Sholin, Plasma Phys. Rep. 22 (1996) 431.
[7] S.I. Krasheninnikov, Contribution Plasma Phys. 36 (1996) 293.
[8] S.I. Krasheninnikov, A.Yu. Pigarov, D.A. Knoll, B. LaBombard, B. Lipschultz, D.J. Sigmar, T.K. Soboleva, J.L. Terry, F. Wising, Phys. Plasma 4 (1997) 1637.
[9] J.L. Terry, B. Lipschultz, A.Yu. Pigarov, S.I. Krasheninnikov, B. LaBombard, D. Lumma, H. Ohkawa, D. Pappas, M. Umansky, Phys. Plasma 5 (1998) 1759.
[10] S.I. Krasheninnikov, A.Yu. Pigarov, D.J. Sigmar, Phys. Lett. A 314 (1996) 285.
[11] A.Yu. Pigarov, S.I. Krasheninnikov, Phys. Lett. A 222 (1996) 251.
[12] D.E. Post, J. Nucl. Mater. 220–222 (1995) 143.
[13] J. Hiskes, Rev. Sci. Instrum. 63 (1992) 2702.
[14] D. Reiter, Chr. May, M. Baelmans, P. Börner, J. Nucl. Mater. 241–243 (1997) 342.
[15] U. Fantz, D. Reiter, B. Heger, D. Coster, J. Nucl. Mater. 290–293 (2001) 367.
[16] K. Sunako, K. Nanri, T. Noguchi, E. Yabe, K. Takayama, Nucl. Instrum. and Meth. B 111 (1996) 151.
[17] A. Tonegawa, K. Kawamura, K. Takayama, N. Ohyavu, T. Watanabe, J. Adv. Sci. 11 (1999) 232.
[18] M. Otsuka, K. Takayama, S. Tanaka, J. Uramoto, S. Aihara, T. Kodama, K. Ishii, Y. Tanaka, in: Proceedings of the Seventh International Conference Phenomena in Ionized Gases, vol. I, Gradjevinska Knjiga Publishing, Beograd, 1966, p. 420.
[19] M. Bacal, G.W. Hamilton, A.M. Bruneteau, H.J. Doucet, Rev. Sci. Instrum. 50 (1979) 719.

[20] M. Bacal, Rev. Sci. Instrum. 71 (2000) 3981.
[21] J.L. Terry, B. Lipshultz, A.Yu. Pigarov, S.I. Krasheninnikov, B. LaBombard, D. Lumma, H. Ohkawa, D. Pappas, M. Umansky, Phys. Plasma 5 (1998) 1759.
[22] D. Lumma, J.L. Terry, B. Lipschultz, Phys. Plasma 4 (1997) 2555.
[23] H. Tawara, Y. Itikawa, H. Nishimura, M. Yoshino, J. Phys. Chem. Ref. Data 19 (1990) 617.